

Modeling and Simulation of Two-Phase Interleaved Boost Converter Using Open-Source Software Scilab/Xcos

Yin Yin Phy, Tun Lin Naing

Abstract—This paper investigated the simulation of two-phase interleaved boost converter (IBC) with free and open-source software Scilab/Xcos. By using interleaved method, it can reduce current stress on components, components size, input current ripple and output voltage ripple. The required mathematical model is obtained from the equivalent circuit of its different four modes of operation for simulation. The equivalent circuits are considered in continuous conduction mode (CCM). The average values of the system variables are derived from the state-space equation to find the equilibrium point. Scilab is now becoming more and more popular among students, engineers and scientists because it is open-source software and free of charge. It gives a great convenience because it has powerful computation and simulation function. The waveforms of output voltage, input current and inductors current are obtained by using Scilab/Xcos.

Keywords—Two-phase boost converter, continuous conduction mode, free and open-source, interleaved method, dynamic simulation.

I. INTRODUCTION

IN recent years, DC-DC converters are widely used in many applications such as renewable energy source and automotive, power factor correction, portable equipments, DC drives and so on [1]-[3]. But the conventional boost converter has many disadvantages such as large output capacitor required to reduce ripple voltage, larger input current ripple and poor efficiency. Interleaved topology is used to solve this problem. Parallel combination of boost converters is used for this technique. And then, the MOSFET switches that must be driven with same switching frequency, $(360/n)$ degree phase shift is called interleaved method. 'n' is the number of parallel circuits. In IBC, the input current is sharing on the components. Therefore, current stress on the components and the components size for high power density can be reduced [4]. Input current ripple and the output voltage ripple can also be reduced by comparing the conventional boost converter. Moreover, the efficiency of two-phase IBC is more than the conventional boost converter.

The Scilab/Xcos is an open-source software for Scientific Computation (OSSC). Xcos contains the graphical editor to design dynamic systems models [5]. It is similar to MATLAB, but it is free and open-source. It is a high-level language, which makes it simple for learning and teaching. It has entered

a fast growing stage for both industrial and educational purposes [6]. Now, it is widely used in secondary and high schools because it includes plenty of mathematical functions [7] and it can also be used to simulate mathematical model of power electronics systems. The Scilab version 6.0.1 can be downloaded from <http://www.scilab.org/>. The largest benefit of Scilab is of course that it is free, easy and fast to install.

Scilab/Xcos has some problems for users because of people unfamiliarity about its internal formalism. Therefore, Liao [8] solved the low computational efficiency by adding little extra costs of the memory to increase the computational speed. Moreover, the Scilab/Xcos can be used in control system for simulation work. For example, Sahana [9] proposed the speed control of DC drive system using Scilab/Xcos. Liu [10] used the Scilab/Xcos as a computational tool to discuss the diagnosis of sensor faults in Aircraft engine control system.

The dynamic response simulation of the two-phase IBC from the differential equations is presented by using MATLAB/Simulink [11], [12]. The two-phase IBC is studied to find the steady-state equation and transfer function from generalized state-space model for N-phase IBC [13]. The IBC is modeled and analyzed using state-space averaging technique in [14]. The modeling of two-phase IBC is presented by using switched-circuit model, input current and output voltage ripple and the output voltage is controlled by using PI controller for fuel cell application [15]. The simulations of these papers are applied in MATLAB/Simulink but MATLAB is a commercial software which is not free. Therefore, this paper presents the dynamic response simulation of two-phase IBC with Scilab/Xcos. Simulation is used to study the dynamic performance of the system without extra cost. When the system undergoes any condition changes, the value of state variables is changed. In this condition, the performance of the system can easily be studied by doing simulation.

This paper presents the modeling and simulation of two-phase IBC using open-source software Scilab/Xcos. Section II describes the circuits operation and mathematical model for two-phase IBC. Section III gives the simulation results and discusses the results. Finally Section IV concludes the paper.

II. MATHEMATICAL MODELING OF TWO-PHASE IBC

The two-phase IBC is illustrated in Fig. 1. The two-phase IBC consists of separate input inductors L_1 and L_2 , Switches S_1 and S_2 , Diodes D_1 and D_2 and the same filter capacitor C at the output. The switches S_1 and S_2 have the same switching

frequency and 180 degree phase shift. The load is represented by a resistor R . The inductor stored and released energy when the switch is ON and OFF. The capacitor is used for filtering of the ripple in the output voltage V_o . The switches S_1 and S_2 are represented by u_1 and u_2 . The possible values of switches are $u_1 \in \{0,1\}$ and $u_2 \in \{0,1\}$ in which 0 and 1 are representing OFF and ON states of the power switches. And the gate signal of switches u_1 and u_2 are applied 180 degree phase shift.

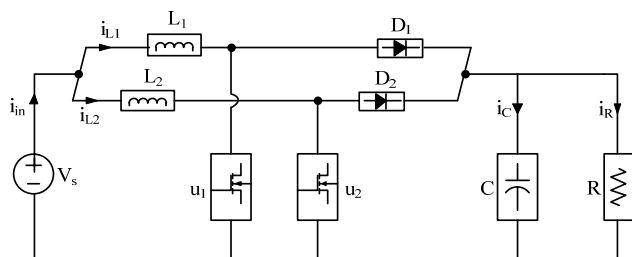


Fig. 1 Circuit diagram of two-phase IBC

A. Switched-Function Model

The system has four modes of operation. The inductor resistance is considered in this paper but the parasitic elements such as on resistance, diode voltage drop and capacitor parasitic resistance are not applied in operation. These modes are operated in CCM. It can be assumed that the values of two input inductors are identical.

Mode 1: $u_1=1$ and $u_2=0$. Fig. 2 illustrates the equivalent circuit of mode 1.

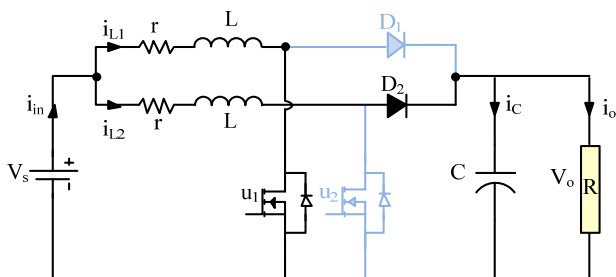


Fig. 2 Equivalent circuit for Mode 1

For equivalent circuit of Mode 1, the differential equations are obtained by applying *Kirchhoff's voltage and current laws*.

$$L \frac{di_{L1}}{dt} = V_s - ri_{L1} \quad (1)$$

$$L \frac{di_{L2}}{dt} = V_s - ri_{L2} - v_o \quad (2)$$

$$C \frac{dv_o}{dt} = i_{L2} - \frac{v_o}{R} \quad (3)$$

Mode 2: $u_1=0$ and $u_2=1$. Fig. 3 shows the equivalent circuit of mode 2.

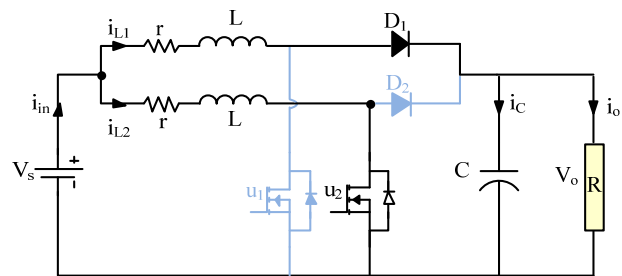


Fig. 3 Equivalent circuit for Mode 2

$$L \frac{di_{L1}}{dt} = V_s - ri_{L1} - v_o \quad (4)$$

$$L \frac{di_{L2}}{dt} = V_s - ri_{L2} \quad (5)$$

$$C \frac{dv_o}{dt} = i_{L1} - \frac{v_o}{R} \quad (6)$$

Mode 3: $u_1=u_2=1$. Fig. 4 illustrates the equivalent circuit of mode 3.

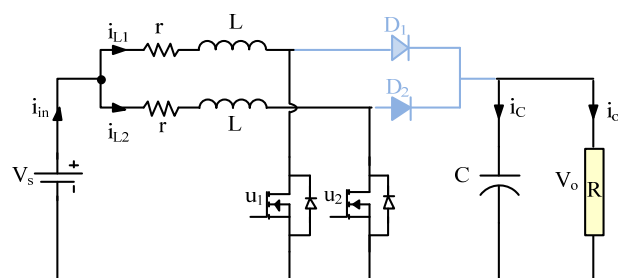


Fig. 4 Equivalent circuit for Mode 3

$$L \frac{di_{L1}}{dt} = V_s - ri_{L1} \quad (7)$$

$$L \frac{di_{L2}}{dt} = V_s - ri_{L2} \quad (8)$$

$$C \frac{dv_o}{dt} = -\frac{v_o}{R} \quad (9)$$

Mode 4: $u_1=u_2=0$. Fig. 5 shows the equivalent circuit of mode 4.

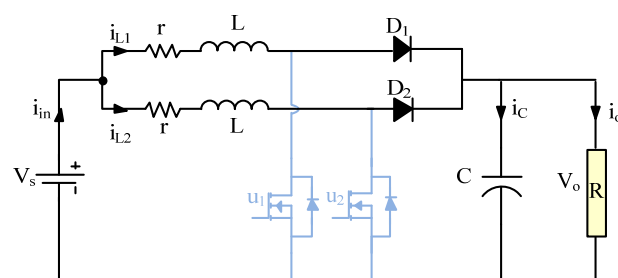


Fig. 5 Equivalent circuit for Mode 4

$$L \frac{di_{L1}}{dt} = V_s - r i_{L1} - v_o \quad (10)$$

$$L \frac{di_{L2}}{dt} = V_s - r i_{L2} - v_o \quad (11)$$

$$C \frac{dv_o}{dt} = i_{L1} + i_{L2} - \frac{v_o}{R} \quad (12)$$

The following differential equations are presented by using switched-function.

$$L \frac{di_{L1}}{dt} = V_s - r i_{L1} - (1 - u_1) v_o \quad (13)$$

$$L \frac{di_{L2}}{dt} = V_s - r i_{L2} - (1 - u_2) v_o \quad (14)$$

$$C \frac{dv_o}{dt} = (1 - u_1) i_{L1} + (1 - u_2) i_{L2} - \frac{v_o}{R} \quad (15)$$

B. Steady-state Equations of the System

The average model of the system is used to obtain the steady-state equations. The average positions \bar{d}_1 and \bar{d}_2 replace the switch positions u_1 and u_2 in (13)-(15).

$$L \frac{d\bar{i}_{L1}}{dt} = V_s - r \bar{i}_{L1} - (1 - \bar{d}_1) \bar{v}_o \quad (16)$$

$$L \frac{d\bar{i}_{L2}}{dt} = V_s - r \bar{i}_{L2} - (1 - \bar{d}_2) \bar{v}_o \quad (17)$$

$$C \frac{d\bar{v}_o}{dt} = (1 - \bar{d}_1) \bar{i}_{L1} + (1 - \bar{d}_2) \bar{i}_{L2} - \frac{\bar{v}_o}{R} \quad (18)$$

whereas, $\bar{u}_1 = \bar{d}_1 \in [0,1]$ and $\bar{u}_2 = \bar{d}_2 \in [0,1]$ are the average positions of the switches. The values of \bar{d}_1 and \bar{d}_2 are the addition of average and small signal value.

$$d_1 = D_1 + \tilde{d}_1 \text{ and } d_2 = D_2 + \tilde{d}_2 \quad (19)$$

If $\tilde{d} \ll D$, \tilde{d} is neglected by using small-signal approximation. \bar{d}_1 and \bar{d}_2 are equal to D in steady-state condition. Therefore, $\bar{d}_1 = \bar{d}_2 = D$.

$$0 = V_s - r i_{L1} - (1 - D) V_o \quad (20)$$

$$0 = V_s - r i_{L2} - (1 - D) V_o \quad (21)$$

$$0 = (1 - D) i_{L1} + (1 - D) i_{L2} - \frac{V_o}{R} \quad (22)$$

Equations (20)-(22) are represented using the following matrix notation.

$$\begin{pmatrix} r & 0 & (1-D) \\ 0 & r & (1-D) \\ (1-D) & (1-D) & -\frac{1}{R} \end{pmatrix} \begin{pmatrix} i_{L1} \\ i_{L2} \\ V_o \end{pmatrix} = \begin{pmatrix} V_s \\ V_s \\ 0 \end{pmatrix} \quad (23)$$

Equation (24) is derived by using (23). It represents the steady-state value of the system.

$$\begin{pmatrix} i_{L1} \\ i_{L2} \\ V_o \end{pmatrix} = \begin{pmatrix} \frac{1}{2R(1-D)^2 + r} \\ \frac{1}{2R(1-D)^2 + r} \\ \frac{2R(1-D)}{2R(1-D)^2 + r} \end{pmatrix} V_s \quad (24)$$

C. Selection of Parameters

The load resistance is calculated from the load power. The inductor value can be chosen by defining the value of inductor current ripple in (25).

$$\Delta i_L = \frac{V_s D}{L f_s} \quad (25)$$

The value of output voltage ripple is defined for finding the value of capacitor in (26).

$$\Delta V_o = \frac{P_o D}{2C V_o f_s} \quad (26)$$

In steady state condition, the value of output voltage for ideal case is obtained from (27).

$$V_o = \frac{1}{1-D} V_s \quad (27)$$

Table I shows the parameters of two-phase IBC. These parameters are obtained from (25)-(27). The value of D is defined 0.5 to obtain the output voltage 24 Volts. The converter switching frequency f_s is 2 kHz in order to operate in CCM. The inductor coil resistance has 0.2.

TABLE I
CONVERTER PARAMETERS

Symbols	Parameters	Values
V_s	Supply voltage	12 [V]
V_o	Output voltage	24 [V]
L_1, L_2	Inductors	2 [mH]
r	Inductor resistance	0.2 [Ω]
C	Capacitor	470 [μ F]
R	Load resistance	18 [Ω]
D	Duty cycle	50%
f_s	Switching frequency	2 [kHz]
P_o	Load power	32 [W]

III. SIMULATION RESULTS AND DISCUSSION

The two-phase IBC is simulated in Scilab/Xcos from average model to validate the steady-state results. The construction of power converter design consumes more time

and cost. Simulation is the best way to study the IBC before the construction.

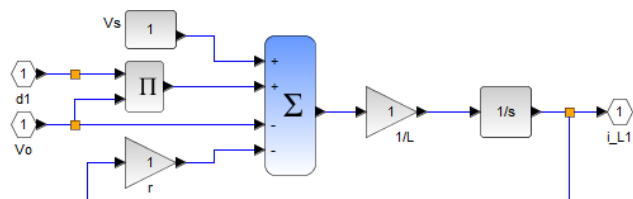


Fig. 6 Block diagram of inductor input current

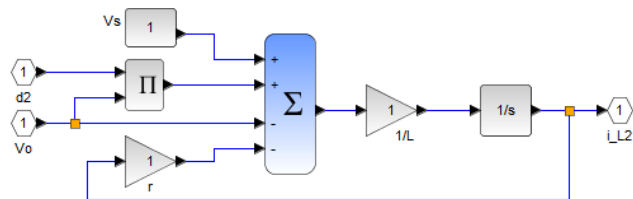


Fig. 7 Block diagram of inductor input current

According to (16), the block diagram for inductor input current (i_{L1}) is shown in Fig. 6. Fig. 7 is the block diagram of

inductor input current (i_{L2}) for (17). Block diagram of output voltage is described in Fig. 8 by using (18).

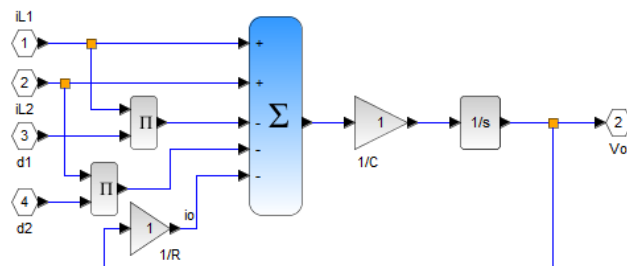


Fig. 8 Block diagram for output voltage

The graphical simulation of two-phase IBC is demonstrated in Fig. 9. The overall system is obtained from the combination of (16)-(18). The converter parameters are used from Table I. The simulation time is defined as 0.05 second. The time period for clock is defined in 1 μ second.

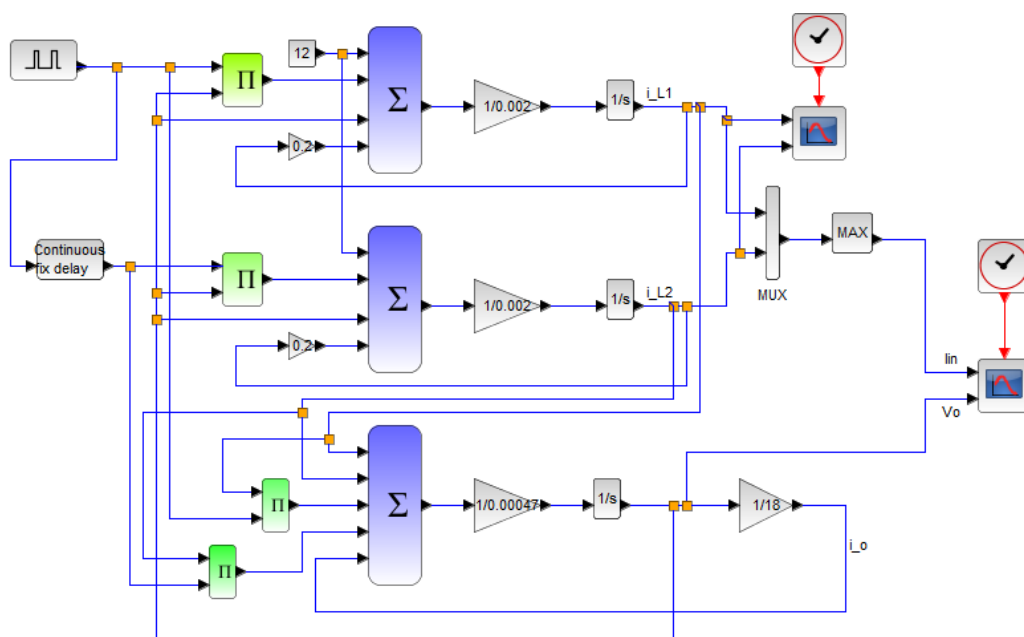


Fig. 9 Graphical simulation of two-phase IBC

TABLE II
STEADY-STATE RESULTS

Equilibrium point	D=0.5	D=0.7
V_o	23.5 [V]	38 [V]
I_{L1}	1.3 [A]	3.5 [A]
I_{L2}	1.3 [A]	3.5 [A]
I_{in}	1.3 [A]	3.5 [A]
Δi_{in}	0.75 [A]	1.05 [A]
Δi_L	1.5 [A]	2.1 [A]

Table II presents the values of the equilibrium point from (24) for $D=0.5$ and 0.7 by using the value of converter parameter in Table I. The waveforms of input current, inductor current and output voltage with duty cycle 50% are illustrated in Figs. 10-14. The inductor current, input current and output voltage waveforms with duty cycle 70% are described in Figs. 15-19.

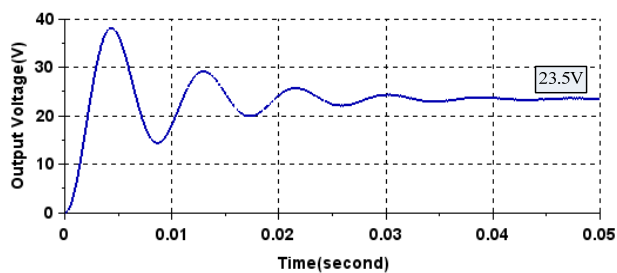


Fig. 10 Output voltage waveform of two-phase IBC at duty cycle 50%

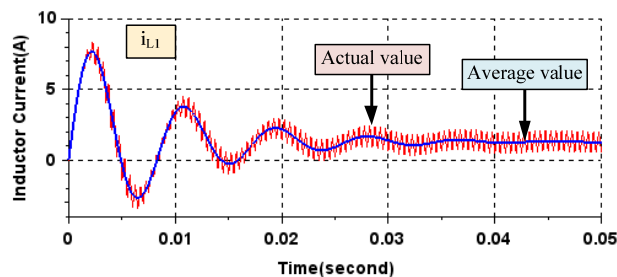


Fig. 11 Inductor current waveform at duty cycle 50%

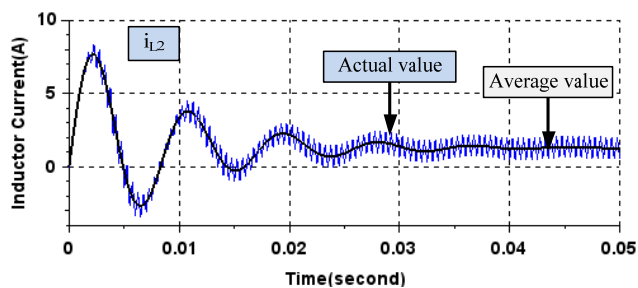


Fig. 12 Inductor current waveform at duty cycle 50%

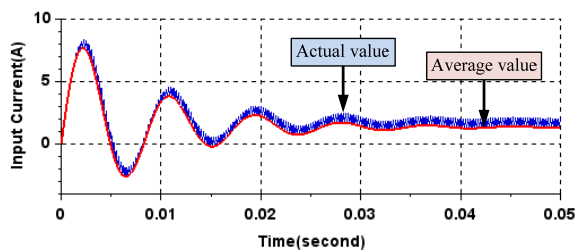


Fig. 13 Input current waveform at duty cycle 50%

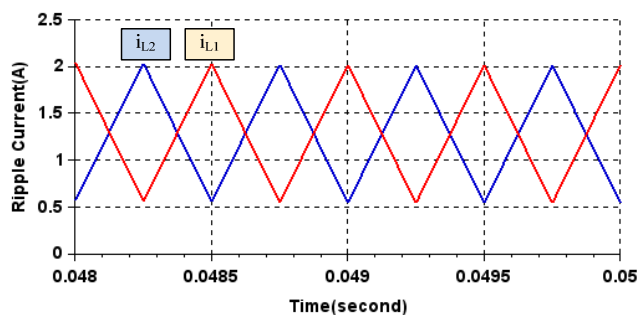


Fig. 14 The steady-state waveforms of inductor current with 180 degree phase shift for $D=0.5$

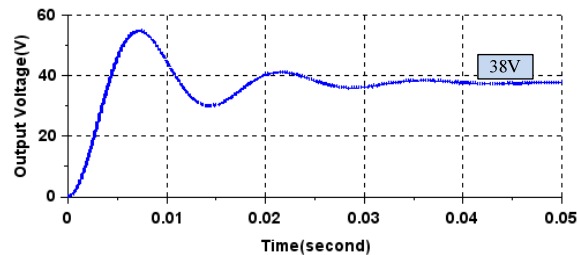


Fig. 15 Output voltage waveform of two-phase IBC for duty cycle 70%

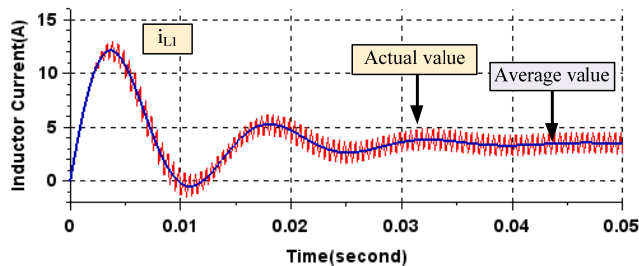


Fig. 16 Inductor current waveform at duty cycle 70%

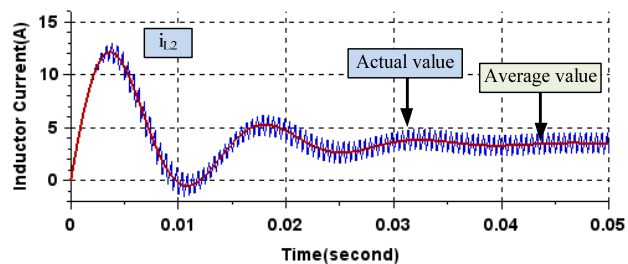


Fig. 17 Inductor current waveform at duty cycle 70%

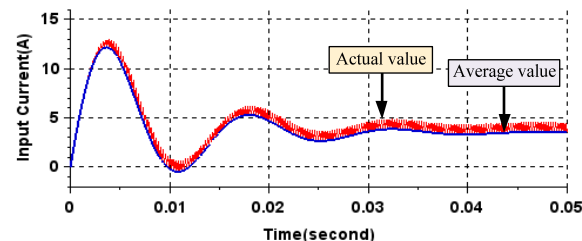


Fig. 18 Input current transient waveform at duty cycle 70%

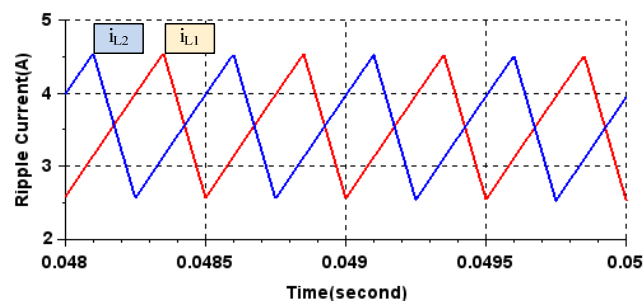


Fig. 19 The steady-state waveforms of inductor current with 180 degree phase shift for $D=0.7$

These simulations describe the dynamic behaviour of the variables v_o , i_{L1} , i_{L2} and i_{in} . The response of the system has

oscillation at the time between 0 to 0.04 seconds and the system reaches the steady state value after 0.04 seconds. The value of input current is high during starting. The value of input current ripple is half of the value of inductor current ripple because the switching frequency is twice. The value of output voltage, inductors current and input current are increased with duty cycle increase but the duty cycle has limitation at the experiment. The value of input current and inductor current ripples are also increased when the duty cycle is increased. The equilibrium point of steady-state value in (24) is the same compare to graphical simulation results. But the output voltage of steady-state value and graphical simulation are different compare to the output voltage from (27) because it is the ideal case (without losses). The inductor current ripple can be reduced by increasing the switching frequency.

IV. CONCLUSIONS

This paper has presented the mathematical modeling and simulation of two-phase IBC. The equilibrium point is presented to validate the graphical simulation results from the average model. The values of the equilibrium point are equal to compare the values from graphical simulation. The switched-function model and the average model are used to analyze the performance of converter and dynamic response simulation. The simulation results are presented by using Scilab/Xcos. The Scilab software gives a great convenience because it is free and open-source software. As future work, it is intended to apply average current mode control method to regulate the output voltage of the system.

REFERENCES

- [1] Mohamed Bougrine, M. Benmiloud, A. Benalia, E. Delaleau, M. Benbouzid, "Load Estimator-based Hybrid Controller Design for Two-Interleaved Boost Converter dedicated to Renewable Energy and Automotive applications", China, 2016.
- [2] Amar Bouafassa, Lazhar Rahmani, Saad Mekhilef, "Design and Real Time Implementation of single phase Boost Power Factor Correction Converter", Malaysia, 2014.
- [3] Walid Emar, Zayed Huneiti, Sofyan Hayajneh, "Analysis, Synthesis and Simulation of compact Two-channel Boost Converter for Portable Equipments operating with a Battery or Solar Cell", 2015.
- [4] Simon Ang, Alejandro Oliva, Power-Switching Converters. Second Edition, Taylor & Francis Group, 2005.
- [5] Zoltan Janik and Katarina Zakova, "Online design of MATLAB/Simulink and Scilab/Xcos block schemes," IEEE, Slovakia, pp. 241-247, September 2011.
- [6] Lijun Wang, Qing Li, Chaonan Tong, Yixin Yin, Jiangyun Li and Siyang Song, "Active Disturbance Rejection Control simulation toolbox in open-source software Scilab/Xcos," IEEE, Beijing, China, pp. 71-76, 2011.
- [7] Scilab: Free and Open-source Software, <http://www.scilab.org/>.
- [8] Haofu Liao, Ping Chen, "Explore a Way of Improving the Computational Efficiency of the Block in SCILAB," IEEE, Beijing, China, pp. 13-16, 2011.
- [9] Sahana M, Sachin. Angadi and A.B.Raju, "Speed Control of Separately Excited DC Motor Using Class A Chopper," IEEE, India, 2016.
- [10] Yue Liu, Daoliang Tan, Ai He and Xi Wang, "UIO-based Diagnosis of Aircraft Engine Control Systems Using Scilab," IEEE, Beijing, China, pp. 64-70, 2011.
- [11] Y.M. Buswig, W.M. Utomo, A.A. Bakar and Z.A. Haron, "State-Space Derivation of an Interleaved Boost Converter," The 2nd Power and Energy Conversion Symposium (PECS), pp. 259-262, 2014.
- [12] N. Jantharamin, L. Zang, "Analysis of Multiphase Interleaved Converter by using State-space Averaging Technique," ECTI-CON 2009 6th international conference publications, May 2009, pp. 288-291.
- [13] H.M. Mallikarjuna Swamy, K.P. Guruswamy and Dr.S.P. Singh, "Design and Implementation of Two Phase Interleaved DC-DC Boost Converter with Digital PID Controller," International Journal of Electrical and Electronics Engineering, Vol. 3, India, 2013.
- [14] S. Somkun, C. Sirisamphanwong and S. Sukchai, "Design and Implementation of an Interleaved Boost DC-DC Converter for PEM Fuel Cells," ISSN: Applied Mechanics and Materials, Vol.666, pp. 87-92, Switzerland, 2014.
- [15] J.S. Anu Rahavi, T. Kanagapriya and Dr.R. Seyezhai, "Design and Analysis of Interleaved Boost Converter for Renewable Energy Source," ICEET, pp. 447-451, India, 2012.